molecular mechanism of differentiation in three-dimensional (3-D) morphology, and bridge between *in vivo* and *in vitro* pharmacological studies.

2. Results and Discussion

2.1. Results

2.1.1. Induction of CYPs in 3-Methylcholanthrene- (3-MC) and Rifampicin-Administered Chimeric Mouse Liver

3-Methylcholanthrene (3-MC) was administered intraperitoneally to groups consisting of three chimeric mice (PXB-mice®), each at a dose of 2 or 20 mg/kg daily for four days. In both the 2 and 20 mg/kg 3-MC-administered groups, the *AUCs* of 3-MC decreased at Day 3 as compared with Day 0 (Figure 1A, Table 1). In the 20 mg/kg group, the *AUC* decreased from 94.4 ng/mL·h on Day 0 to 35.4 ng/mL·h on Day 3; the difference was significant (0.4-fold; $p < 0.01$; Figure 1B, Table 1). The reductions in *AUC* were accompanied by decreases in C_{max} (Table 1). Rifampicin was also administered intraperitoneally to groups of three mice, at dose levels of 0.1 or 10 mg/kg daily for four days. After the four days of administration, the *AUCs* of rifampicin decreased in both 0.1 (0.7-fold, Figure 1C, Table 1) and 10 mg/kg-administered groups (0.6-fold, Figure 1D, Table 1), but the difference was not significant. The decreases in C_{max} were confirmed in both groups.

Figure 1. Plasma concentrations of 3-MC or Refampicin in the *in vivo* study. Plasma concentrations of 3-MC (**A**,**B**) and rifampicin (**C**,**D**) were measured on the first (Day 0) and the last (Day 3) day of administration. Open circles indicate data on Day 0. Closed circles indicate data on Day 3. Data are mean ± S.D.

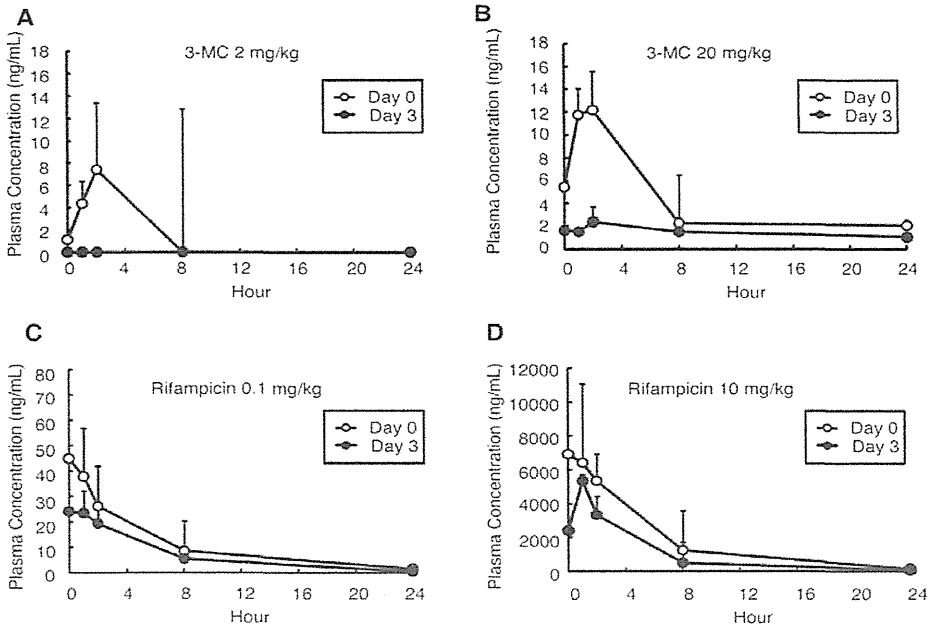

Table 1. PK profile in *in vivo* study.

Inducer	Dose (mg/kg)	Day	*AUC* [(1)] (Ratio to Day 0) (ng/mL·h)	$T_{1/2}$ (h)	C_{max} [(1)] (ng/mL)	T_{max} (h)
3-MC	2	0	44.2 ± 0.0	2.1	7.4 ± 0.0	2.0
	-	3	0.0 ± 0.0 (0.0)	-	-	-
	20	0	94.4 ± 20.8	8.6	12.2 ± 4.3	2.0
	-	3	35.4 ± 21.3 ** (0.4)	9.1	2.4 ± 0.3	2.0
Rifampicn	0.1	0	236.8 ± 76.6	3.1	45.0 ± 19.2	0.5
	-	3	154.9 ± 47.6 (0.7)	3.5	24.1 ± 8.7	0.5
	10	0	40,186.5 ± 9,088.3	3.0	6,926.0 ± 4,653.4	0.5
	-	3	22,125.3 ± 6,222.4 (0.6)	2.0	5,353.3 ± 1,122.5	1.0

[(1)] mean ± S.D.; ** $p < 0.01$.

mRNA expression levels were determined by real-time quantitative RT-PCR (qRT-PCR) using liver samples collected at 24 h after the last administration on Day 4. The mRNA expression levels of h*CYP1A1*, h*CYP1A2*, and h*CYP3A4* were normalized to the expression levels of human *glyceraldehyde 3-phosphate dehydrogenase* (h*GAPDH*) (Table 2). Although the chimeric mouse livers contained mouse hepatocytes (<30%), real-time qRT-PCR determined the gene expression levels of only human hepatocytes but not mouse hepatocytes because the primers were human-specific. The mRNA expression levels of h*CYP1A1* and h*CYP1A2* increased in the 20 mg/kg 3-MC-administered group, and the change in h*CYP1A1* was significant as compared with the control group (7.3-fold, $p < 0.05$, Table 2). The mRNA expression levels of h*CYP3A4* increased significantly in the 10 mg/kg rifampicin-administered group (5.1-fold, $p < 0.05$, Table 2).

Table 2. mRNA expression levels in *in vivo* study.

Group	Dose (mg/kg)	h*CYP1A1*/h*GAPDH* [(1)] (Ratio to the Control)	h*CYP1A2*/h*GAPDH* [(1)] (Ratio to the Control)	h*CYP3A4*/h*GAPDH* [(1)] (Ratio to the Control)
Corn oil	-	0.112 ± 0.041 (1.0)	2.576 ± 1.081 (1.0)	2.471 ± 0.804 (1.0)
3-MC	2	0.156 ± 0.037 (1.4)	3.091 ± 0.850 (1.2)	-
	20	0.812 ± 0.217 * (7.3)	5.666 ± 3.283 (2.2)	-
Rifampicin	0.1	-	-	2.718 ± 0.375 (1.1)
	10	-	-	12.519 ± 6.296 * (5.1)

[(1)] mean ± S.D.; * $p < 0.05$.

Protein expression levels of human CYPs were determined by Western blotting using microsomal fractions isolated from the mouse liver. The protein expression level of hCYP1A2 increased significantly in the 20 mg/kg 3-MC group (1.5-fold, $p < 0.05$, Figure 2, Table 3), and the protein expression level of hCYP3A4 in the 10 mg/kg rifampicin group increased significantly (2.2-fold; $p < 0.05$) as compared with the control group (Figure 2, Table 3).

Figure 2. Protein expression levels in the *in vivo* study. Changes in hCYP1A2 expression induced by four days of 3-MC administration (**A**) and in hCYP3A4 expression induced by four days of rifampicin administration (**B**) are shown.

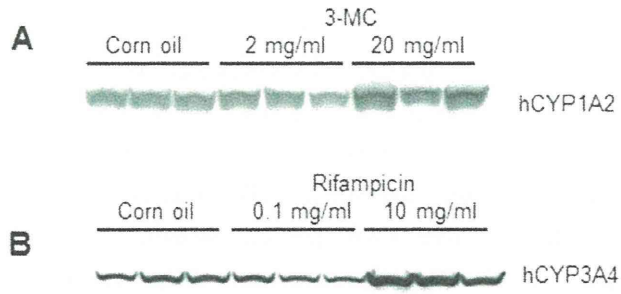

Table 3. Protein expression levels in *in vivo* study.

Group	Dose (mg/kg)	hCYP1A2 [(1)] (Ratio to the Control)	hCYP3A4 [(1)] (Ratio to the Control)
Corn oil	-	6,906.7 ± 488.0	2169.0 ± 527.7
3-MC	2	6,220.7 ± 1,082.8 (0.9)	-
	20	10,389.0 ± 1,943.0 * (1.5)	-
Rifampicin	0.1	-	1,798.3 ± 372.1 (0.8)
	10	-	4,796.3 ± 1,198.0 * (2.2)

[(1)] mean ± S.D.; * $p < 0.05$.

2.1.2. Regional Distribution of hCYP1A2 and 3A4 Expression with 3-MC and Rifampicin Administration

The localization of hCYP1A2 and 3A4 was immunohistochemically determined using cryosections of livers from untreated and 3-MC- or rifampicin-administered chimeric mice. Both hCYP1A2 and 3A4 were located in the centrilobular, but not the periportal area in control chimeric mouse livers (Figure 3A–C,G–I). After four days of 3-MC or rifampicin administration, the expression of these CYPs expanded to the periportal area (Figure 3D–F,J–L).

2.1.3. *In Vitro* Induction of CYPs in 3-MC- or Rifampicin-Treated Human Hepatocytes

Fresh human hepatocytes (PXB-cells) were isolated from chimeric mice by a two-step collagenase perfusion method, and prepared as monolayer and spheroid cultures. In the present study, the chimeric mouse hepatocytes contained <10% mouse hepatocytes. Similar to the *in vivo* study, real-time qRT-PCR determined the gene expression levels of only human hepatocytes but not mouse hepatocytes because the primers were human specific. The baseline mRNA expression levels of hCYP1A1, hCYP1A2, and hCYP3A4 in monolayer and spheroid cultures were confirmed at 72 and 96 h post inoculation as compared with the control (immediately after isolation). For hCYP1A1, mRNA expression levels were maintained at more than 10% of the *in vivo* control in both monolayer and spheroid cultures at 72 and 96 h (Figure 4A, $p < 0.05$). For hCYP1A2 and hCYP3A4, mRNA expression levels decreased to less than 1% of the control in the monolayer culture, while in the spheroid culture, expression was maintained at around 10% of the control at 72 and 96 h (Figure 4A,

$p < 0.05$), suggesting the 3-D culture maintained human hepatocytes in more differentiated phase than monolayer culture.

Figure 3. Double immunohistochemistry for human cytokeratin 8/18 (CK8/18) and hCYP1A2, and CK8/18 and hCYP3A4 in chimeric mouse livers treated with inducers (3-MC, rifampicin). hCK8/18 (**A**,**D**,**G**,**J**) was visualized with FITC (green color), and hCYP3A4 (**B**,**E**) and hCYP1A2 (**H**,**K**) were visualized with Texas Red (red color). The overlays of hCK8/18 and hCYP3A4 or hCK8/18 and hCYP1A2 are shown in (**C**,**F**,**I**,**L**). (**A**–**C**,**G**–**I**) was derived from non-treated animals. (**D**–**F**) was derived from rifampicin-treated animals and (**J**–**L**) was derived from 3-MC-treated animals. H, human hepatocyte-region; M, mouse hepatocyte-region. CV, central vein; PV, portal vein. Bar, 100 μm. Magnifications of (**A**–**E**) and (**F**–**K**) are same as those of (**F**) and (**L**), respectively.

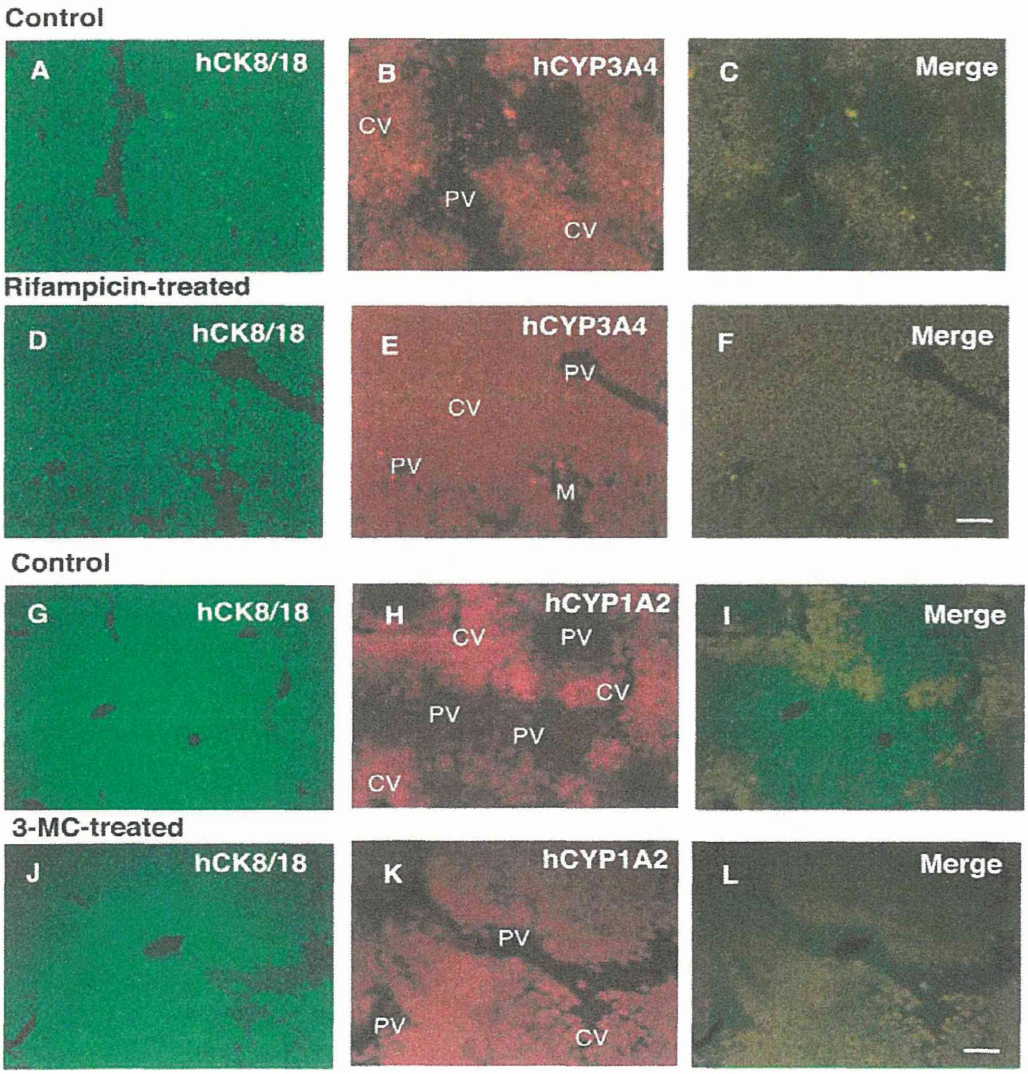

Figure 4. mRNA expression levels in the *in vitro* study. The baseline mRNA expression levels of h*CYP1A1*, h*CYP1A2* and h*CYP3A4* in monolayer culture and spheroid culture of human hepatocytes after inoculation are shown in (**A**); Changes in the value of h*CYP1A1*/h*GAPDH*, h*CYP1A2*/h*GAPDH*, and h*CYP3A4*/h*GAPDH* by inducers are shown in (**B**,**C**) and (**D**), respectively. Data are mean ± S.D. * $p < 0.05$; ** $p < 0.01$.

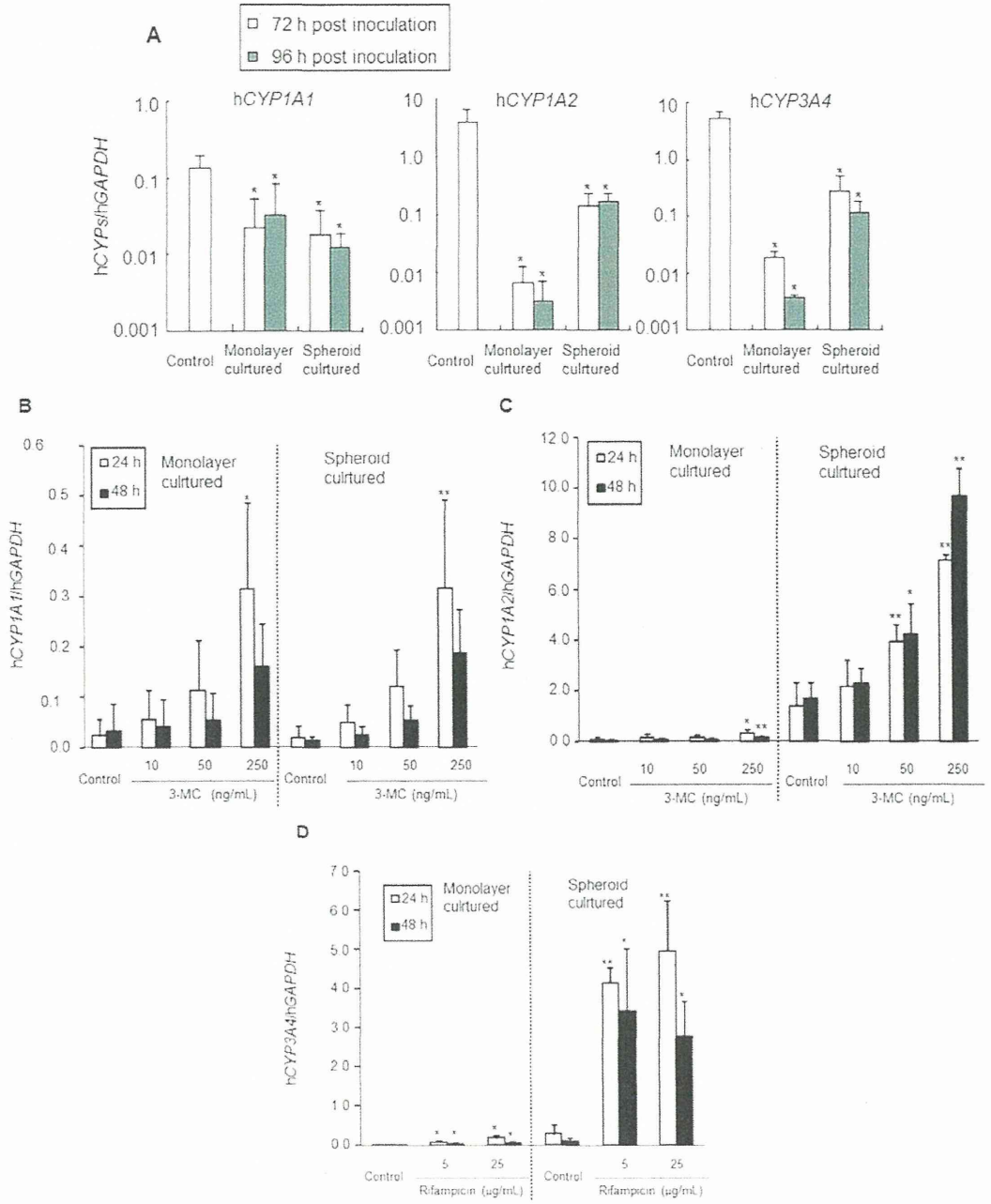

Isolated human hepatocytes were incubated with 3-MC at 10, 50, or 250 ng/mL, or with rifampicin at 5 or 25 μg/mL. The incubation times were set at 24 (72 h after inoculation) and 48 h (96 h after inoculation). To evaluate enzyme induction, mRNA expression levels of h*CYP1A1*, h*CYP1A2*, and h*CYP3A4* were determined by real-time qRT-PCR and normalized to the expression level of h*GAPDH*. The normalized mRNA expression levels of h*CYP1A1* increased in a concentration-dependent manner in

both monolayer and spheroid cultures, and the induction ratios were quite similar between them. Significant differences were observed in monolayer (14.3-fold, $p < 0.05$) and spheroid cultures (17.3-fold, $p < 0.01$) treated with 250 ng/mL 3-MC at 24 h (Table 4, Figure 4B). Although the expression levels of *CYP1A2* were less than 0.1-fold lower in monolayer culture than spheroid culture, the mRNA expression levels of h*CYP1A2* also increased in a concentration-dependent manner in both monolayer culture and spheroid culture, and the induction ratios were similar between them. Significant differences were observed in monolayer cultures treated with 250 ng/mL 3-MC at both 24 (4.9-fold, $p < 0.05$) and 48 h (4.9-fold, $p < 0.01$), and in monolayer cultures treated with 50 ng/mL 3-MC at both 24 (2.8-fold, $p < 0.01$) and 48 h (2.5-fold, $p < 0.05$) and with 250 ng/mL 3-MC at both 24 (5.1-fold, $p < 0.01$) and 48 h (5.8-fold, $p < 0.01$; Table 4, Figure 4C).

Although the mRNA expression levels of *CYP3A4* were less than 0.1-fold lower in monolayer culture than spheroid culture, similar to *CYP1A2* expression, concentration-dependent increases were confirmed at 24 and 48 h in both monolayer and spheroid cultures. All of these increases were significant compared with the control, and the induction ratio was higher in spheroid culture than monolayer culture (Table 4, Figure 4D).

2.2. Discussion

The present study was conducted to demonstrate the potential usefulness of chimeric mice with humanized livers in both *in vivo* and *in vitro* enzyme induction studies. In the *in vivo* study, a significant decrease in *AUC* of 3-MC was induced by four days 3-MC administration (20 mg/kg), which was associated with a significant increase in h*CYP1A1* mRNA expression and hCYP1A2 protein expression. *AUC* decreases were observed at 2 mg/kg in the 3-MC group (but not significant) although the expression levels of mRNA (h*CYP1A1* and h*CYP1A2*) and protein (hCYP1A2) did not increase significantly after dosing. These results show that although 3-MC is known to be metabolized by CYP1A [11], we expected that up-regulation of mRNA or protein of, not only CYP1A1 and 1A2, but also other metabolic enzymes or transporters might contribute to the apparent auto-induction by 3-MC. There was no significant difference in *AUC* levels between the control and rifampicin-treated groups; however, the *AUC* decreased by about one-half in the 10 mg/kg rifampicin group, and this change was associated with a significant increase in h*CYP3A4* mRNA and protein expression levels. Although the exact mechanism is not known, chronic dosing of rifampicin induces its own metabolism [12]. In addition, the *AUCs* in 10 mg/kg of rifampicin-administered group were similar to the *AUC* at steady state (*AUCss*) of human treated with a therapeutic dose of rifampicin (22,400 to 35,300 ng·h/mL [13]). Rifampicin is a potent and selective activator of the human nuclear pregnane X receptor (PXR). It has been reported that there are significant differences in ligand recognition by PXR between rodents and humans [14]. Although the chimeric mice retain less than 30% mouse hepatocytes, decreases in *AUC* might have occurred by PXR-related induction in human hepatocytes but not in mouse hepatocytes. Recently we reported that CYP3A4 and CYP2C subfamilies were induced by treatment of the PXB mice with 50 mg/kg rifampicin for four days. However treatment with 10 mg/kg decreased only the *AUC* of the CYP3A4 substrate, and did not affect the *AUC* of CYP2C substrates [15]. These data suggest that induction of CYP3A4 might contribute to the *AUC* decrease of rifampcin. On the

other hand, as 3-MC induces mouse Cyp1a1 and hCYP1A [11], the Cyp1a1 induction in less than 30% mouse hepatocytes in the chimeric liver might contribute to 3-MC auto-induction.

The protein induction of hCYP1A2 and hCYP3A4 in the chimeric mice was supported by the immunohistochemistry results. In the *in vivo* situation, there is morphological, biochemical, molecular, and functional heterogeneity between periportal and pericentral hepatocytes [16–20]. CYP3A and CYP1A2 are expressed in pericentral, but not in periportal, hepatocytes in rodent and human liver lobules [19,20]. It has been reported that administering phenobarbital to rats induces the expression of CYP3a1 in periportal hepatocytes [20]. In the present study, we demonstrated that *in vivo* treatment of human hepatocytes with rifampicin and 3-MC induced hCYP3A4 and hCYP1A2 expression in periportal hepatocytes of the chimeric mice, resulting in uniform expression of these enzymes throughout the liver lobules. These data are consistent with our previous study showing induction of CYP3A4 in rifampicin-treated chimeric mice [21]. These results demonstrated that chimeric mice with humanized liver are appropriate for evaluating enzyme induction in human hepatocytes, based on *in vivo* exposure levels of the inducer and tissue levels.

Recently, we demonstrated that these chimeric mice may be useful for supplying fresh human hepatocytes on demand, thus, promising high and stable phase I enzyme and glucuronidation activities [10]. In the present *in vitro* study, we also demonstrated the feasibility of conducting 24- or 48-h enzyme induction studies in both monolayer and spheroid cultures using human hepatocytes freshly isolated from the chimeric mice. Given the scarcity of fresh human hepatocytes for conducting *in vitro* studies, fresh human hepatocytes isolated from chimeric mice may be a viable alternative. Additionally, it is possible to reproducibly conduct *in vitro* enzyme induction studies with fresh human hepatocytes derived from the same donor and to compare results of *in vitro* and *in vivo* studies using cells from the same donor.

For *in vitro* CYP induction study, hepatocytes are typically cultured in monolayer conditions. However, because CYP mRNAs, proteins, and activities decline immediately during monolayer culture, induction levels have been estimated at much lower levels (less than 1%) than *in vivo* levels [8]. In the present study, we compared *CYP1A1*, *1A2*, and *3A4* mRNA expression levels between hepatocytes just after isolation and monolayer- or spheroid-cultured hepatocytes at 72 and 96 h. *CYP1A2* and *3A4* mRNA expression levels in hepatocytes in both culture conditions decreased; however, they were maintained at more than 10-fold higher levels in spheroid cultures than in monolayer cultures, although *CYP1A1* mRNA expression levels were similar between hepatocytes in the two conditions. Based on these results, hepatocytes in the spheroid culture apparently maintain their differentiated state better than those in monolayer culture. Thus, we consider the spheroid-cultured hepatocytes to be hepatocytes with differentiation characteristics between those *in vivo* and in monolayer culture. *In vitro* CYP induction studies were performed in monolayer and spheroid cultures. Induction responsiveness and induction ratios of *CYP1A1* were similar between the two conditions. On the other hand, sensitivities of *CYP1A2* were higher in spheroid culture (50 ng/mL) than monolayer culture (250 ng/mL), however, the induction ratios were quite similar between them at the highest dose (3-MC 250 ng/mL). The sensitivity of *CYP3A4* was also similar (5 μg/mL), but induction ratios were higher in spheroid than monolayer cultures. From these results, sensitivities and induction ratios were similar or somewhat higher in spheroid than monolayer cultures.

Table 4. mRNA expression levels in *in vitro* study.

Item	Group	Monolayer Culture		Spheroid Culture	
		24 h [(1)] (Ratio to the Control)	48 h [(1)] (Ratio to the Control)	24 h [(1)] (Ratio to the Control)	48 h [(1)] (Ratio to the Control)
h*CYP1A1*/h*GAPDH*	Control	0.022 ± 0.033 (1.0)	0.033 ± 0.054 (1.0)	0.018 ± 0.021 (1.0)	0.013 ± 0.007 (1.0)
	3-MC 10 ng/mL	0.053 ± 0.060 (2.4)	0.038 ± 0.056 (1.2)	0.047 ± 0.035 (2.6)	0.023 ± 0.018 (1.8)
	3-MC 50 ng/mL	0.112 ± 0.101 (5.1)	0.053 ±0.053 (1.6)	0.120 ± 0.073 (6.6)	0.053 ± 0.028 (4.2)
	3-MC 250 ng/mL	0.314 ± 0.170 * (14.3)	0.158 ± 0.086 (4.9)	0.315 ± 0.175 ** (17.3)	0.186 ± 0.087 (14.9)
h*CYP1A2*/h*GAPDH*	Control	0.007 ± 0.006 (1.0)	0.003 ± 0.004 (1.0)	0.139 ± 0.091 (1.0)	0.168 ± 0.062 (1.0)
	3-MC 10 ng/mL	0.015 ± 0.011 (2.3)	0.004 ± 0.004 (1.4)	0.215 ± 0.106 (1.6)	0.228 ± 0.056 (1.4)
	3-MC 50 ng/mL	0.017 ± 0.008 (2.5)	0.006 ± 0.004 (1.8)	0.392 ± 0.069 ** (2.8)	0.423 ± 0.117 * (2.5)
	3-MC 250 ng/mL	0.033 ± 0.012 * (4.9)	0.015 ± 0.004 ** (4.9)	0.713 ± 0.023 ** (5.1)	0.967 ± 0.111 ** (5.8)
h*CYP3A4*/h*GAPDH*	Control	0.019 ± 0.004 (1.0)	0.004 ± 0.000 (1.0)	0.278 ± 0.240 (1.0)	0.116 ± 0.070 (1.0)
	Rifampicin 5 μg/mL	0.075 ± 0.044 * (4.0)	0.040 ± 0.020 * (10.9)	4.138 ± 0.405 ** (14.9)	3.421 ± 1.601 * (29.4)
	Rifampicin 25 μg/mL	0.187 ± 0.061 * (9.8)	0.055 ± 0.025 * (15.1)	4.952 ± 1.294 ** (17.8)	2.770 ± 0.907 * (23.8)

[(1)] mean ± S.D.; * $p < 0.05$; ** $p < 0.01$.

Information from these *in vivo* and *in vitro* enzyme induction studies using human hepatocytes from the same donor may be useful in advancing predictions of enzyme induction in humans. For example, in the present study, 12.2 ng/mL of 3-MC in the *in vivo* study (20 mg/kg, Day 0) was sufficient to induce a significant decrease in *AUC* of 3-MC and a significant increase in h*CYP1A1* mRNA expression and hCYP1A2 protein expression. On the other hand, the *in vitro* study revealed that 250 ng/mL of 3-MC was needed to induce a significant increase in h*CYP1A1* mRNA in both monolayer and spheroid cultures, and 250 and 50 ng/mL 3-MC was needed to induce a significant increase of h*CYP1A2* mRNA in the monolayer and spheroid cultures, respectively, as shown above. The sensitivity to 3-MC was higher in spheroid than monolayer cultures for both hCYP1A1 and 1A2. The sensitivity of *CYP1A1* and *1A2* mRNA expression levels to 3-MC was in the following sequence: *in vivo* > spheroid ≥ monolayer. However, the sensitivity of CYP3A4 for rifampicin was similar between *in vivo* and *in vitro*.

3. Experimental Section

3.1. Materials

3-MC and rifampicin were purchased from Sigma-Aldrich (St. Louis, MO, USA). All other chemicals and vehicle were of analytical grade or the highest commercially available quality.

3.2. Generation of Chimeric Mice with Humanized Livers

The present study was approved by the Ethics Committees of PhoenixBio. To generate chimeric mice with humanized livers, cryopreserved human hepatocytes, which had been donated with informed consent, were purchased from BD Bioscience, Woburn, MA, USA (10YF, 10-year-old female Caucasian). Chimeric mice with humanized livers (PXB-mice®) were generated using a previously reported method [2]. Briefly, human hepatocytes were transplanted into the spleen of uPA/SCID mice at two to four weeks of age. From three weeks after the transplantation, 2 μL of blood was collected from the mice once per week and the concentration of human albumin (hAlb) in the blood was determined based on latex agglutination immunonephelometry to estimate the replacement index (RI, repopulation ratio of human hepatocytes in the host mouse liver). The correlation between hAlb concentration and the RI was established in a previous report [2]. In the present study 152 mice were transplanted with human hepatocytes and 74 mice (48.7%) showed >6 mg/mL hAlb (RI > 70%). The specifications of the chimeric mice used for the *in vivo* study were as follows: male, 12–14 weeks old, 6.3–10.9 mg/mL hAlb in the blood (RI > 70%), and 14.2–22.8 g body weight (Table 5). For the *in vitro* study, chimeric mice with 6.2–14.8 mg/mL hAlb in the blood (RI > 70%) were used to isolate human hepatocytes (Table 6).

Table 5. Chimeric mice used in the *in vivo* study.

Donor Cells	Group	Dose (mg/kg)	No. of Animals	Age (weeks)	hAl in Blood [(1)] (Min–Max) (mg/mL)	Body Weight [(1)] (Min–Max) (g)	RI *,[(1)] (%)
10YF	Corn oil	-	3	12–13	8.2 ± 2.4 (6.7–10.9)	18.7 ± 1.2 (17.4–19.8)	79 ± 8 (74–89)
	3-MC	2	3	12–14	8.3 ± 2.1 (6.7–10.6)	19.7 ± 1.9 (17.5–21.3)	80 ± 7 (74–88)
		20	3	13–14	8.2 ± 2.1 (6.5–10.5)	17.8 ± 3.7 (14.2–21.5)	80 ± 8 (73–88)
	Rifampicin	0.1	3	12–13	7.5 ± 1.0 (6.4–8.4)	19.6 ± 3.7 (15.5–22.8)	77 ± 5 (72–81)
		10	3	13–14	7.6 ± 1.1 (6.3–8.5)	19.6 ± 2.4 (17.5–22.2)	77 ± 5 (72–81)

[(1)] mean ± S.D.; * expected RI. RI calculated by the blood hAlb levels using the formula of the correlation curve $y = 30.4 \ln(x) + 16.0$ ($r^2 = 0.88$) in which x and y represent r^2 and hAlb level, respectively.

Table 6. Chimeric mice used in the *in vitro* study.

Donor Cells	hAl in Blood (mg/mL)	RI * (%)	Cell Yield (×10^7 Cells)	Viability (%)
10YF	14.8	98	4.5	75.1
	11.0	89	8.1	65.3
	8.1	80	10.9	80.3
	6.2	72	10.2	65.8

* expected RI. RI calculated by the blood hAlb levels using the formula of the correlation curve $y = 30.4 \ln(x) + 16.0$ ($r^2 = 0.88$) in which x and y represent r^2 and hAlb level, respectively.

3.3. In Vivo *CYP Induction Study*

3-MC and rifampicin were suspended in corn oil. Three chimeric mice per group were intraperitoneally administered corn oil, 2, or 20 mg/kg 3-MC, or 0.1 or 10 mg/kg rifampicin daily for four days (10 mL/kg). Blood was collected from the treated mice at 0.5, 1, 2, 8, and 24 h post first (Day 0) and last dosing (Day 3), and the plasma was used to determine concentrations of 3-MC and rifampicin. After the last blood sampling, these mice were euthanized under anesthesia, and the livers were harvested for the isolation of total RNA and microsomes.

3.4. Measurement of 3-MC and Rifampicin Concentrations in Mouse Plasma

To compare the effects of inducers between *in vivo* and *in vitro* studies, the plasma concentrations of 3-MC and rifampicin were measured by Sekisui Medical Co., Ltd. (Tokyo, Japan). A plasma sample (2 μL) was mixed well with 2 μL of acetonitrile and 60 μL of internal control solution, and centrifuged (22,000 ×*g*, 4 °C, 10 min). The supernatant was then applied to liquid chromatography-tandem mass spectrometry (LC-MS/MS; MDS SCIEX; Applied Biosystems, Foster City, CA, USA). Area under the curves (*AUCs*) were calculated based on the concentrations of 3-MC and rifampicin.

3.5. Immunohistochemistry

To evaluate the distribution of hCYP1A2 and hCYP3A4 in the chimeric mouse liver lobules following administration of 3-MC (20 mg/kg) and rifampicin (50 mg/kg) once daily for four days, immunohistochemistry was conducted using liver specimens from the chimeric mice. These liver specimens were derived as reported previously [2]. Chimeric mice with nine-month-old male Caucasian (9MM) and 12-year-old male Caucasian (12YM) donor cells were used to evaluate the distribution of hCYP1A2 and hCYP3A4, respectively. Livers were removed at 24 h after the last administration of inducers and then processed for double immunohistochemistry. Livers from non-treated mice were used as controls (Table 7). Cryosections (5 μm thick) were incubated with anti-human-specific cytokeratin 8 and 18 (hCK8/18) antibodies (ICN Pharmaceuticals, Inc, Aurora, OH, USA), and rabbit anti-human CYP1A2 or CYP3A4 polyclonal antibodies (Affiniti Research Products, Ltd., Exeter, UK). Immunoreactions for hCK8/18 and hCYP1A2 or hCYP3A4 were visualized with FITC-conjugated anti-mouse IgG (Fc) (Pierce Biotechnology, Inc. Rockford, IL, USA) and Texas Red-conjugated anti-rabbit IgG (H + L) (Vector Laboratories, Inc. Burlingame, CA, USA), respectively. These antibodies were confirmed to have human-specific reactivity (data not shown).

Table 7. Donor information and details of treatment of the liver samples for immunohistochemistry.

Donor Cells	Group	Dose (mg/kg)	No. of Animals	Age (weeks)	hAl in Blood (mg/mL)	Body Weight (g)	RI * (%)
9MM	Control	-	6	12–14	1.4–5.7	9.0–21.8	1–57
	3-MC	20	3	12–13	1.4–10.7	12.9–13.8	6–76
12YM	Control	-	6	10–14	0.03–5.1	5.1–22.8	41–89
	Rifampicin	50	3	16–18	0.07–4.6	13.5–16.5	45–49

* expected RI. RI calculated by the blood hAlb levels using the formula of the correlation curve $y = 13.3 \ln(x) + 48.6$ ($r^2 = 0.76$) for 9MM and in $y = 19.3 \ln(x) - 227.0$ ($r^2 = 0.63$) for 12YM in which x and y represent r^2 and hAlb level, respectively.

3.6. Preparation of Fresh Human Hepatocytes from Chimeric Mice

Human hepatocytes were isolated from chimeric mice by a two-step collagenase perfusion method as reported previously [10]. After completion of the perfusion, liver cells were disaggregated in CMF-HBSS containing 10% bovine albumin, 10 mM Hepes, and 10 mg/mL gentamycin. The disaggregated cells were centrifuged three times (50 ×g, 2 min). The pellet was suspended in medium consisting of Dulbecco's modified Eagle's medium (DMEM) with 10% fetal bovine serum (FBS), 20 mM Hepes, 44 mM $NaHCO_3$, and antibiotics (100 IU/mL penicillin G and 100 μg/mL streptomycin) (DMEM10). Cell number and viability were estimated by the trypan blue exclusion test. The cell number (yield) of isolated viable hepatocytes was 4.5×10^7–10.9×10^7 cells/mouse, and the viability was 65.3%–80.3% (Table 6).

3.7. In Vitro *CYP Induction Study*

The isolated human hepatocytes (PXB-cells) in DMEM10 medium were immediately inoculated on uncoated 24-well plates (Corning Life Science, Tewksburry, MA, USA) for the monolayer culture and Matrigel-coated 24-well plates (BD Biosciences, San Jose, CA, USA) for the spheroid culture at a cell density of 5×10^4 cells/cm^2 [22]. At 5 h post inoculation, the medium was changed to remove dead cells. Then, 19 h later, the medium was changed to serum-free medium (HHM; Toyobo, Osaka, Japan) and the cells were cultured for 24 h. The induction began after the completion of the formation of both the monolayer culture on uncoated 24-well plates and the spheroid culture on Matrigel-coated 24-well plates. The medium was changed to HHM containing the solvent control, 10, 50, or 250 ng/mL 3-MC, or 5 or 25 μg/mL rifampicin. At 24 h (72 h post inoculation) and 48 h post induction (96 h post inoculation), cells were harvested in RLT buffer (Qiagen K.K., Tokyo, Japan) to isolate total RNA for determining hCYP1A1, hCYP1A2, and hCYP3A4 mRNA expression levels by real-time qRT-PCR and stored at −80 °C until use.

3.8. Determination of mRNA Expression Levels by Real-Time qRT-PCR

Total RNA was isolated from the harvested hepatocytes or chimeric mouse livers and then treated with DNase (Qiagen, Tokyo, Japan), purified using the RNase-Free DNase Set (Qiagen, Tokyo, Japan) and the RNeasy Mini Kit (Qiagen, Tokyo, Japan). mRNA expression levels of h*CYP1A1*, h*CYP1A2*, and h*CYP3A4* were quantified by real-time qRT-PCR. cDNA was synthesized using 1 μg RNA, PowerScript reverse transcriptase (Clontech, Mountain View, CA, USA), and random primers (Life Technologies Corp., Carlsbad, CA, USA) according to the manufacturer's protocol, and was subjected to real-time qRT-PCR. Genes were amplified with a set of gene-specific primers (Table 8) and the SYBR Green PCR mix in a PRISM 7700 Sequence Detector (Life Technologies Corporation, Carlsbad, CA, USA). We confirmed that these primers were capable of amplifying human, but not mouse genes. Levels of PCR products were monitored continuously during amplification by measuring the increases in intensity of SYBR Green 1 that bound to the double-stranded DNA. The PCR conditions consisted of an initial denaturation step at 95 °C for 10 min, followed by 40 cycles of 95 °C for 15 s, and 60 °C for 1 min. Results were calculated by the comparative threshold cycle (C_t) method, as described previously [23]. To normalize the human mRNA expression levels in total RNA samples, the expression of human CYP mRNA was divided by the value for h*GAPDH* mRNA individually, because the extracted total RNA sample contained varying amounts of total RNA derived from mouse tissue.

Table 8. Primers used in this study.

Target Gene	Primer	Sequence
hCYP1A1	Forward	TCAACCATGACCAGAAGCTA
	Reverse	AAGATAATCACCTTCTCACTTAACAC
hCYP1A2	Forward	GCTTCTACATCCCCAAGAAAT
	Reverse	ACCACTTGGCCAGGACT
hCYP3A4	Forward	ACTGCCTTTTTTGGGAAATA
	Reverse	GGCTGTTGACCATCATAAAAG
hGAPDH	Forward	GGAGTCAACGGATTTGGT
	Reverse	AAGATGGTGATGGGATTTCCA

3.9. Western Blotting

Microsomal fractions were isolated from chimeric mice livers [24], aliquots of which (25 μg of protein) were loaded on 10% SDS-polyacrylamide gels, electrophoresed, and transferred to nitrocellulose membranes. The membranes were incubated with antibodies against hCYP1A2 (Sekisui Medical Co., Ltd., Tokyo, Japan) and hCYP3A4 (Sekisui Medical Co., Ltd., Tokyo, Japan) and visualized using the ECL Western Blotting Detection System (Amersham Biosciences Corp., Piscataway, NJ, USA). The intensity of the detected color on the nitrocellulose membrane was measured using the ImageJ software (ver. 1.43; NIH, Bethesda, MD, USA).

3.10. Statistical Analyses

Statistical differences were evaluated with a homogeneity of variance test (Bartlett's test), followed by Dunnett's and Steel's tests.

4. Conclusions

We report here for the first time, CYP induction levels determined for inducers *in vivo* and *in vitro* using cells from the same donor. The comparison between *in vivo* and *in vitro* data using the chimeric mice can provide valuable information for predicting the CYP-inducing abilities of new drug candidates, both quantitatively and qualitatively. The present study demonstrated that a chimeric mouse with a humanized liver is a unique tool for evaluating enzyme induction, and we propose using the chimeric mice in both *in vivo* and *in vitro* enzyme induction studies for advancing predictions of enzyme-inducing effects in humans.

Conflicts of Interest

The authors declare no conflict of interest.

References

1. Mercer, D.F.; Schiller, D.E.; Elliott, J.F.; Douglas, D.N.; Hao, C.; Rinfret, A.; Addison, W.R.; Fischer, K.P.; Churchill, T.A.; Lakey, J.R.; *et al.* Hepatitis C virus replication in mice with chimeric human livers. *Nat. Med.* **2001**, *7*, 927–933.
2. Tateno, C.; Yoshizane, Y.; Saito, N.; Kataoka, M.; Utoh, R.; Yamasaki, C.; Tachibana, A.; Soeno, Y.; Asahina, K.; Hino, H.; *et al.* Near completely humanized liver in mice shows human-type metabolic responses to drugs. *Am. J. Pathol.* **2004**, *165*, 901–912.
3. Katoh, M.; Matsui, T.; Nakajima, M.; Tateno, C.; Kataoka, M.; Soeno, Y.; Horie, T.; Iwasaki, K.; Yoshizato, K.; Yokoi, T. Expression of human cytochromes P450 in chimeric mice with humanized liver. *Drug Metab. Dispos.* **2004**, *32*, 1402–1410.
4. Katoh, M.; Matsui, T.; Okumura, H.; Nakajima, M.; Nishimura, M.; Naito, S.; Tateno, C.; Yoshizato, K.; Yokoi, T. Expression of human phase II enzymes in chimeric mice with humanized liver. *Drug Metab. Dispos.* **2005**, *33*, 1333–1340.

5. Okumura, H.; Katoh, M.; Sawada, T.; Nakajima, M.; Soeno, Y.; Yabuuchi, H.; Ikeda, T.; Tateno, C.; Yoshizato, K.; Yokoi, T. Humanization of excretory pathway in chimeric mice with humanized liver. *Toxicol. Sci.* **2007**, *97*, 533–538.
6. Azuma, H.; Paulk, N.; Ranade, A.; Dorrell, C.; Al-Dhalimy, M.; Ellis, E.; Strom, S.; Kay, M.A.; Finegold, M.; Grompe, M. Robust expansion of human hepatocytes in *Fah*$^{-/-}$/*Rag2*$^{-/-}$/*Il2rg*$^{-/-}$ mice. *Nat. Biotechnol.* **2007**, *25*, 903–910.
7. Hasegawa, M.; Kawai, K.; Mitsui, T.; Taniguchi, K.; Monnai, M.; Wakui, M.; Ito, M.; Suematsu, M.; Peltz, G.; Nakamura, M.; *et al.* The reconstituted "humanized liver" in TK-NOG mice is mature and functional *Biochem. Biophys. Res. Commun.* **2011**, *405*, 405–410.
8. Nishimura, M.; Yokoi, T.; Tateno, C.; Kataoka, M.; Takahashi, E.; Horie, T.; Yoshizato, K.; Naito, S. Induction of human CYP1A2 and CYP3A4 in primary culture of hepatocytes from chimeric mice with humanized liver. *Drug Metab. Pharmacokinet.* **2005**, *20*, 121–126.
9. Yoshitsugu, H.; Nishimura, M.; Tateno, C.; Kataoka, M.; Takahashi, E.; Soeno, Y.; Yoshizato, K.; Yokoi, T.; Naito, S. Evaluation of human *CYP1A2* and *CYP3A4* mRNA expression in hepatocytes from chimeric mice with humanized liver. *Drug Metab. Pharmacokinet.* **2006**, *21*, 465–474.
10. Yamasaki, C.; Kataoka, M.; Kato, Y.; Kakuni, M.; Usuda, S.; Ohzone, Y.; Matsuda, S.; Adachi, Y.; Ninomiya, S.; Itamoto, T.; *et al. In vitro* evaluation of cytochrome P450 and glucuronidation activities in hepatocytes isolated from liver-humanized mice. *Drug Metab. Pharmacokinet.* **2010**, *25*, 539–550.
11. Jiang, W.; Wang, L.; Kondraganti, S.R.; Fazili, I.S.; Couroucli, X.I.; Felix, E.A.; Moorthy, B. Disruption of the gene for *CYP1A2*, which is expressed primarily in liver, leads to differential regulation of hepatic and pulmonary mouse *CYP1A1* expression and augmented human *CYP1A1* transcriptional activation in response to 3-methylcholanthrene *in vivo*. *J. Pharmacol. Exp. Ther.* **2010**, *335*, 369–379.
12. Loos, U.; Musch, E.; Jensen, J.C.; Mikus, G.; Schwabe, H.K.; Eichelbaum, M. Pharmacokinetics of oral and intravenous rifampicin during chronic administration. *Klin. Wochenschr.* **1985**, *63*, 1205–1211.
13. Polk, R.E.; Brophy, D.F.; Israel, D.S.; Patron, R.; Sadler, B.M.; Chittick, G.E.; Symonds, W.T.; Lou, Y.; Kristoff, D.; Stein, D.S. Pharmacokinetic Interaction between amprenavir and rifabutin or rifampin in healthy males. *Antimicrob. Agents Chemother.* **2001**, *45*, 502–508.
14. LeCluyse, E.L.; Pregnane X receptor: Molecular basis for species differences in CYP3A induction by xenobiotics. *Chem. Biol. Interact.* **2001**, *134*, 283–289.
15. Hasegawa, M.; Tahara, H.; Inoue, R.; Kakuni, M.; Tateno, C.; Ushiki, J. Investigation of drug-drug interactions caused by human pregnane X receptor-mediated induction of CYP3A4 and CYP2C subfamilies in chimeric mice with a humanized liver. *Drug Metab. Dispos.* **2012**, *40*, 474–480.
16. Katz, N.; Teutsch, H.F.; Sasse, D.; Jungermann, K. Heterogeneous distribution of glucose-6-phosphatase in microdissected periportal and perivenous rat liver tissue. *FEBS Lett.* **1977**, *76*, 226–230.
17. Gebhardt, R.; Ebert, A.; Bauer, G. Heterogeneous expression of *glutamine synthetase* mRNA in rat liver parenchyma revealed by *in situ* hybridization and Northern blot analysis of RNA from periportal and perivenous hepatocytes. *FEBS Lett.* **1988**, *241*, 89–93.

18. Chen, G.; Baron, J.; Duffel, M.W. Enzyme- and sex-specific differences in the intralobular localizations and distributions of aryl sulfotransferase IV (tyrosine-ester sulfotransferase) and alcohol (hydroxysteroid) sulfotransferase a in rat liver. *Drug Metab. Dispos.* **1995**, *23*, 1346–1353.
19. Ratanasavanh, D.; Beaune, P.; Morel, F.; Flinois, J.P.; Guengerich, F.P.; Guillouzo, A. Intralobular distribution and quantitation of cytochrome P-450 enzymes in human liver as a function of age. *Hepatology* **1991**, *13*, 1142–1151.
20. Bühler, R.; Lindros, K.O.; Nordling, A.; Johansson, I.; Ingelman-Sundberg, M. Zonation of cytochrome P450 isozyme expression and induction in rat liver. *Eur. J. Biochem.* **1992**, *204*, 407–412.
21. Emoto, C.; Yamato, Y.; Sato, Y.; Ohshita, H.; Katoh, M.; Tateno, C.; Yokoi, T.; Yoshizato, K.; Iwasaki, K. Non-invasive method to detect induction of CYP3A4 in chimeric mice with a humanized liver. *Xenobiotica* **2008**, *38*, 239–248.
22. Thissen, J.P.; Pucilowska, J.B.; Underwood, L.E. Differential regulation of insulin-like growth factor I (IGF-I) and IGF binding protein-1 messenger ribonucleic acids by amino acid availability and growth hormone in rat hepatocyte primary culture. *Endocrinology* **1994**, *134*, 1570–1576.
23. Asahina, K.; Sato, H.; Yamasaki, C.; Kataoka, M.; Shiokawa, M.; Katayama, S.; Tateno, C.; Yoshizato, K. Pleiotrophin/heparin-binding growth-associated molecule as a mitogen of rat hepatocytes and its role in regeneration and development of liver. *Am. J. Pathol.* **2002**, *160*, 2191–2205.
24. Sugihara, K.; Kitamura, S.; Yamada, T.; Ohta, S.; Yamashita, K.; Yasuda, M.; Fujii-Kuriyama, Y. Aryl hydrocarbon receptor (AhR)-mediated induction of xanthine oxidase/xanthine dehydrogenase activity by 2,3,7,8-tetrachlorodibenzo-*p*-dioxin. *Biochem. Biophys. Res. Commun.* **2001**, *281*, 1093–1099.

OPEN ACCESS Freely available online

PLOS ONE

Isolation and Characterization of Highly Replicable Hepatitis C Virus Genotype 1a Strain HCV-RMT

Masaaki Arai[1,2], Yuko Tokunaga[2], Asako Takagi[1,2], Yoshimi Tobita[2], Yuichi Hirata[2], Yuji Ishida[3], Chise Tateno[3], Michinori Kohara[2]*

1 Advanced Medical Research Laboratory, Mitsubishi Tanabe Pharma Corporation, Kanagawa, Japan, **2** Department of Microbiology and Cell Biology, Tokyo Metropolitan Institute of Medical Science, Tokyo, Japan, **3** PhoenixBio Co., Ltd., Hiroshima, Japan

Abstract

Multiple genotype 1a clones have been reported, including the very first hepatitis C virus (HCV) clone called H77. The replication ability of some of these clones has been confirmed *in vitro* and *in vivo*, although this ability is somehow compromised. We now report a newly isolated genotype 1a clone, designated HCV-RMT, which has the ability to replicate efficiently in patients, chimeric mice with humanized liver, and cultured cells. An authentic subgenomic replicon cell line was established from the HCV-RMT sequence with spontaneous introduction of three adaptive mutations, which were later confirmed to be responsible for efficient replication in HuH-7 cells as both subgenomic replicon RNA and viral genome RNA. Following transfection, the HCV-RMT RNA genome with three adaptive mutations was maintained for more than 2 months in HuH-7 cells. One clone selected from the transfected cells had a high copy number, and its supernatant could infect naïve HuH-7 cells. Direct injection of wild-type HCV-RMT RNA into the liver of chimeric mice with humanized liver resulted in vigorous replication, similar to inoculation with the parental patient's serum. A study of virus replication using HCV-RMT derivatives with various combinations of adaptive mutations revealed a clear inversely proportional relationship between *in vitro* and *in vivo* replication abilities. Thus, we suggest that HCV-RMT and its derivatives are important tools for HCV genotype 1a research and for determining the mechanism of HCV replication *in vitro* and *in vivo*.

Citation: Arai M, Tokunaga Y, Takagi A, Tobita Y, Hirata Y, et al. (2013) Isolation and Characterization of Highly Replicable Hepatitis C Virus Genotype 1a Strain HCV-RMT. PLoS ONE 8(12): e82527. doi:10.1371/journal.pone.0082527

Editor: Stephen J. Polyak, University of Washington, United States of America

Received June 17, 2013; **Accepted** October 24, 2013; **Published** December 16, 2013

Funding: This study was supported in part by a grant from the Ministry of Education, Culture, Sports, Science and Technology of Japan and a grant from the Ministry of Health, Labour and Welfare of Japan. The funders had no role in study design, data collection and analysis, decision to publish, or preparation of the manuscript.

Competing Interests: Masaaki Arai and Asako Takagi are employees of Mitsubishi Tanabe Pharma Corporation and Yuji Ishida and Chise Tateno are employees of PhoenixBio Co., Ltd. The other authors have no conflicts of interest to declare. This does not alter the authors' adherence to all the PLOS ONE policies on sharing data and materials.

* E-mail: kohara-mc@igakuken.or.jp

Introduction

Hepatitis C virus (HCV) is an enveloped positive-strand RNA virus that belongs to the Flaviviridae family [1]. HCV infection is a major cause of chronic hepatitis, liver cirrhosis, and hepatocellular carcinoma. With over 170 million people currently infected worldwide [2], HCV represents a growing public health burden despite the launch of new antiviral medications that directly inhibit virus replication [3,4].

Since HCV was first identified in 1989 as the major cause of non-A and non-B hepatitis [5], great progress has been made in understanding the life cycle of HCV. The first propagation system for this disease agent was an *in vivo* chimpanzee model [6,7,8]. Although that system is still occasionally used as a pivotal animal model for some drugs, chimeric mice with humanized liver that is generated by transplanting human hepatocytes [9,10] are more popular now because of the low cost and the absence of ethical concerns associated with the use of chimpanzees. For *in vitro* research, establishment of an HCV replicon system [11,12] was an important achievement that allowed research into the function of individual non-structural viral proteins. However, the entire viral life cycle remains enigmatic because no structural proteins are needed in this system. Some reports have been published about full-length replicons with structural proteins in addition to non-structural proteins, although little [13] or no [14,15] secretion of infectious virions was observed, which may have been partly due to adaptive mutations. Another breakthrough was made with the discovery of a genotype 2a Japan fulminant hepatitis (JFH)-1 strain that soon became well known for its vigorous replication as a replicon with no adaptive mutations [16]. JFH-1 can also infect and propagate in cultured cells as a virus, especially in HuH-7 cells or their derivatives [17–19]. After the discovery of JFH-1, two methods were available for the investigation of how viral proteins other than those of HCV genotype 2a function during their entire life cycle. The first method was only for structural proteins and involved making a hybrid of the structural region of the clone of interest and the non-structural regions of JFH-1 for efficient replication [20–22]. The other method utilized the entire viral genome sequence of genotype 1 and made them infectious to HuH-7 derivative cells by introducing known adaptive mutations [23,24] or enhancing replication with a casein kinase inhibitor [25]; however, their replication abilities were somehow compromised. In this study, we report the isolation of a new genotype 1a strain from a patient's serum sample that was highly infectious to human hepatocyte-transplanted chimeric mice, as the viral titer in the blood of the mice was higher than 10^8 copies/ml. We

evaluated its replication abilities in four replication systems: subgenomic replicon, virus, *in vitro* infection, and *in vivo* infection. The new HCV clone, which was designated HCV-RMT (GenBank accession number, AB520610), was different from other genotype 1a clones because it did not require any artificially introduced adaptive mutations for the establishment of replicon cells. With these features, our newly cloned HCV-RMT may be a useful tool for investigating the entire life cycle of genotype 1 HCV.

Materials and Methods

Ethics Statement

This study was carried out in strict accordance with both the *Guidelines for Animal Experimentation* of the Japanese Association for Laboratory Animal Science and the recommendations in the *Guide for the Care and Use of Laboratory Animals* of the National Institutes of Health. All protocols were approved by the ethics committee of Tokyo Metropolitan Institute of Medical Science.

Cloning and Sequencing

Acute-phase serum from an HCV genotype 1a-infected patient, HCG9 (purchased from International Reagents Corp., Kobe, Japan; discontinued), was supplemented with 0.1 μg/μl yeast tRNA, and total RNA was extracted using ISOGEN-LS (Nippon Gene, Tokyo, Japan) according to the manufacturer's information. Purified RNA (1 μg) was reverse transcribed using LongRange Reverse transcriptase (QIAGEN, Valencia, CA, USA) and a 21-mer oligonucleotide (antisense sequence 9549-9569 of HCV-H77: GenBank accession number AF011751) as the primer. The first PCR amplification was carried out with the generated cDNA and Phusion DNA polymerase (Finnzymes, Vantaa, Finland) using sense primers corresponding to nucleotides 9-28, 2952-2972, and 5963-5979 (numbers correspond to the HCV-H77 sequence) and antisense primers corresponding to nucleotides 4038-4054, 7042-7057, and 9549-9569. The second nested PCR amplification was carried out with these three products using sense primers corresponding to nucleotides 23-43, 2967-2987, and 5981-6000 and antisense primers corresponding to nucleotides 4018-4033, 7016-7035, and 9534-9554. For the cloning of terminals, total RNA was purified from non-supplemented HCG9 serum. The 5′ terminus was amplified with a 5′ RACE system kit (Invitrogen, Carlsbad, CA, USA) using one-fourth of the purified total RNA from 100 μl serum and antisense primers corresponding to nucleotides 255–273 for the first PCR and 241–261 for the second nested PCR. For the 3′ terminus, the poly(A) tail was added to the 3′ terminus of the same amount of RNA with poly(A) polymerase (Takara Bio Inc., Shiga, Japan). Reverse transcription and PCR amplification of this region were carried out using oligo-d(T) as the reverse primer for both reactions and primers corresponding to nucleotides 9385-9408 for PCR.

All fragments were subcloned using a TOPO cloning kit (Invitrogen), and sequences yielding 10 or more clones per fragment were determined with the Big Dye Terminator mix and ABIprism3100 (Applied Biosystems, Foster City, CA, USA). The consensus sequence was determined by accepting the most frequent nucleotide at each position.

Construction and RNA transcription

To generate full-length viral RNA, the HCV-RMT sequence, which has an endogenous *Xba*I site, was mutated to a silent mutation (T3941C) using a QuikChangeII kit (Stratagene, La Jolla, CA, USA) and cloned into the *Hind*III site of pBR322 with an additional T7 promoter at the beginning and an *Xba*I site at the end. Replicon construction of HCV-RMT was performed by replacing nucleotides 390-3419 of HCV-RMT with the neomycin resistance gene, encephalomyocarditis virus internal ribosome entry site (EMCV-IRES), and an additional start codon at the beginning of the NS3 region. For RNA generation, plasmids were digested with *Xba*I and used as a template for RNA transcription using a RiboMax kit (Promega, Madison, WI, USA).

Cells and Electroporation

HuH-7 cells were cultured in DMEM-GlutaMax-I (Invitrogen) supplemented with 10% fetal bovine serum, penicillin, and streptomycin (Invitrogen). Replicon cells were maintained in the same medium supplemented with 300 μg/ml G418 (Invitrogen). Cells were passaged three times a week at a split of four times. Electroporation of replicon RNA and G418 selection were performed as previously described [11,12]. The cured replicon cell clone (HuH7-K4) was established as previously described [13]. Briefly, authentic subgenomic replicon cells were treated with 1000 IU interferon-α (Mochida Pharmaceutical Co., Ltd., Tokyo, Japan) for 2 months and cloned using the limiting dilution method.

Quantification of HCV RNA

Total RNA was purified from 1 μl chimeric mouse serum using SepaGene RV-R (Sanko Junyaku, Tokyo, Japan), and total RNA was prepared from cells or liver tissues using the acid guanidium thiocyanate-phenol-chloroform extraction method. Quantification of HCV RNA copy number with real-time RT-PCR was performed using an ABI 7700 system (Applied Biosystems) as described previously [26].

Western blot analysis and immunofluorescence analysis

Western blot analysis was carried out according to the conventional semi-dry blot method. Cells were lysed with lysis buffer (10 mM Tris-HCl, pH 7.4 containing 1% sodium dodecyl sulfate, 0.5% Nonidet P-40, 150 mM NaCl, 0.5 mM EDTA, and 1 mM dithiothreitol). Protein (10 μg) from each sample was separated with SDS-PAGE through a 10% polyacrylamide gel and transferred to a polyvinylidene difluoride membrane, Immobilon-P (Millipore, Billerica, MA, USA). HCV NS3 protein was detected with 5 μg/ml anti-NS3 polyclonal antibody (R212) as described previously [27]. HCV NS5B protein and β-actin were detected with 0.5 μg/ml anti-NS5B polyclonal antibody (ab35586; Abcam, Cambridge, UK) and 0.2 μg/ml anti-β-actin monoclonal antibody (AC-15; Sigma-Aldrich, St. Louis, MO, USA), respectively.

For immunofluorescence analysis, cells were washed twice with PBS(−) and fixed with 100% methanol (chilled at −80°C) at −20°C for 20 min. Fixed cells were treated with PBS(−) supplemented with 1% BSA and 2.5 mM EDTA overnight at 4°C. Blocking and antibody treatments were also carried out in the same buffer. Stained cells were viewed with a laser scanning confocal microscope LSM510 (Carl Zeiss, Oberkochen, Germany). HCV core proteins were detected with 5 μg/ml α-HCV core monoclonal antibody (31-2) prepared in our laboratory [28].

In vitro infection and α-CD81 blocking

HuH7-K4 cells were seeded at 6×10^4 cells/well onto a φ10-mm coverglass in a 48-well plate 24 h before inoculation with 240 μl culture medium. At 72 h post-inoculation, cells were fixed with 100% methanol (chilled to −80°C) for 20 min at −20°C. HCV core proteins were detected with 5 μg/ml α-HCV core antibody 31-2. Fluorescent-positive foci were counted under fluorescence microscopy, and the focus-forming units (ffu) per milliliter of supernatant were calculated.

For α-CD81 blocking, HuH7-K4 cells were pre-treated with a serial dilution of α-CD81 antibody (JS81, BD Pharmingen, San Diego, CA, USA) or normal mouse IgG_1 (BD Pharmingen) as an isotype control for 1 h before inoculation.

Drug treatment

#11 cells (5,000 cells/well), which were established using the single cell cloning of HCV-RMTtri-electroporated cells, were seeded in 96-well tissue culture plates and cultivated overnight. Serial dilutions of cyclosporin A (Fluka Chemie, Buchs, Switzerland) or interferon-α (Mochida Pharmaceutical Co., Ltd.) were added. After incubation for 72 h, total RNA was extracted from cells, and HCV-RNA was quantified as described above. The experiments were carried out in triplicate.

In vivo infection

Chimeric mice with humanized liver (PhoenixBio, Hiroshima, Japan) were infected with 10 μl patient serum HCG9 by intravenous injection. For analysis of infectivity of the HCV genome clone, mice were directly injected with 30 μg of the generated RNAs into five to six sites in the liver during abdominal surgery. Blood samples were collected once a week and used for quantification of HCV copy number.

Results

Cloning of a new HCV genotype 1a strain from the serum of an HCG9-infected mouse

We first infected chimeric mice with humanized liver with patient serum HCG9. HCV in HCG9 serum was classified as genotype 1a with RT-PCR genotyping and showed a relatively high replication ability in the patient and a comparable or better replication ability in the chimeric mice (Figure 1A). In one infected mouse, the HCV copy number in blood reached 1×10^9/ml (data not shown). Using two mice with blood titers of 1×10^8 and 1×10^9 copies/ml, we cloned HCV sequences with the standard PCR amplification method using HCV-H77 as a source of primer sequences. Except for some length variations in the poly-pyrimidine tract region, we found no differences in HCV sequences from mouse blood with titers of 1×10^8 and 1×10^9 copies/ml when considering major consensus nucleotides at all sites (GenBank accession number AB520610). The HCV sequences were identical to the HCV sequence cloned from HCG9 serum itself (data not shown). We designated this sequence as HCV-RMT. Its homology to the HCV-H77 strain was 92.8% for nucleotides and 95.1% for amino acids. The *in vivo* replication ability was confirmed with direct injection of the generated HCV-RMT RNA genome into livers of the chimeric mice. Blood titers were comparable to infection with parental HCG9 serum (Figure 1B). JFH-1 infection resulted in a 2-log lower blood titer than HCV-RMT when the same procedure was used.

Establishment of subgenomic replicon cells with the HCV-RMT strain

Next, we generated an authentic subgenomic replicon RNA construct using the HCV-RMT sequence and used it to establish replicon cells. Only two colonies appeared after electroporation with 30 μg of the HCV-RMT replicon RNA and G418 selection. One of these colonies had a reasonable HCV subgenome copy number, and thus, we propagated it and determined the sequence of the subgenome. The determined consensus sequence of the subgenome had three mutations from the wild type: two were located in the NS3 region (E1056V and E1202G), and one was in the NS5A region (A2199T) (Figure 1C). We introduced these mutations into the HCV-RMT replicon sequence as a single mutation or combination of mutations and identified the mutations that were responsible for colony formation (Figure 1D). The most influential single mutation was E1202G in the NS3 region, although a combination of all three mutations (designated RMTtri) resulted in the best replication ability. Interestingly, western blot analysis and HCV genome quantification revealed that the amount of HCV viral components in cells was independent of the colony-forming ability and seemed to be negatively affected by the most beneficial adaptive mutation (E1202G) (Figure 1E).

The HCV-RMT RNA genome with adaptive mutations was maintained in HuH-7 cells

Next, we assessed the *in vitro* replication abilities of HCV-RMT derivatives as a viral genome rather than a replicon. We introduced adaptive mutation(s) into the HCV-RMT sequence (Figure 2A) and electroporated the *in vitro*-generated RNAs into Huh-7.5.1 and HuH7-K4 cells. Electroporated cells were passaged every 2 to 4 days depending on their confluency, and sampling of cells for quantification of the HCV RNA genome was carried out at each passage. The amounts of HCV-RMTtri and JFH-1 were maintained at $\geq1\times10^5$ copies/μg total RNA, in contrast to wild-type HCV-RMT, which was eliminated rapidly (Figure 2B). Additionally, different cell preferences were observed with the two strains of HCV: JFH-1 replicated well in Huh-7.5.1 cells compared to HCV-RMTtri, but the opposite was seen in HuH7-K4 cells. These tendencies were observed repeatedly (Figure S1). Different replication abilities were also observed among derivatives of the HCV-RMT strain and corresponded to the colony-forming ability of the replicon constructs (Figure 2C). Immunostaining of HCV core proteins revealed that many cells (19.2%) were stained in HCV-RMTtri RNA electroporated cells compared to small number cells (0.98%) were stained in HCV-RMT with E1202G mutated RNA electroporated cells (Figure 2D).

The supernatant of HCV-RMTtri-replicating cells was infectious to naïve HuH7-K4 cells

To assess the infectivity of HCV-RMTtri, we used the limiting dilution method to establish clone number 11 (#11) cells in which HCV-RMTtri was highly replicating. The percent of cells expressing the HCV core protein in #11 cells was 75.3±5.0% as seen with immunostaining, whereas the percent of parental cells expressing the HCV core protein was 6.3±2.2% (Figure 3A; the value was calculated as an average of ten observed areas). The cells maintained 1×10^8 copies/μg total RNA of the HCV-RMTtri RNA genome. We collected the supernatants from #11 cells 2 months after cloning and HuH7-K4 cells carrying JFH-1 2 months after establishment. To evaluate infectivity, we added these supernatants to the medium of naïve HuH7-K4 cells. Cells were stained with anti-HCV core protein antibody 3 days later, and we observed core protein-positive cell foci per 0.78 cm^2 in at least triplicate wells (Figure 3B). The calculated ffu of the supernatant was 160 ffu/ml, which was similar to that of H77 with artificially introduced adaptive mutations. This infection was inhibited by anti-CD81 antibody in a similar concentration-dependent manner as *in vitro* infection of JFH-1 (Figure 3C). #11 cells were also useful for evaluating anti-HCV agents such as cyclosporin A and interferon-α (Figure 3D) when 5,000 cells/well (96 well plate) of #11 cells were treated with inhibitors for 72 h beginning 1 day after passaging.

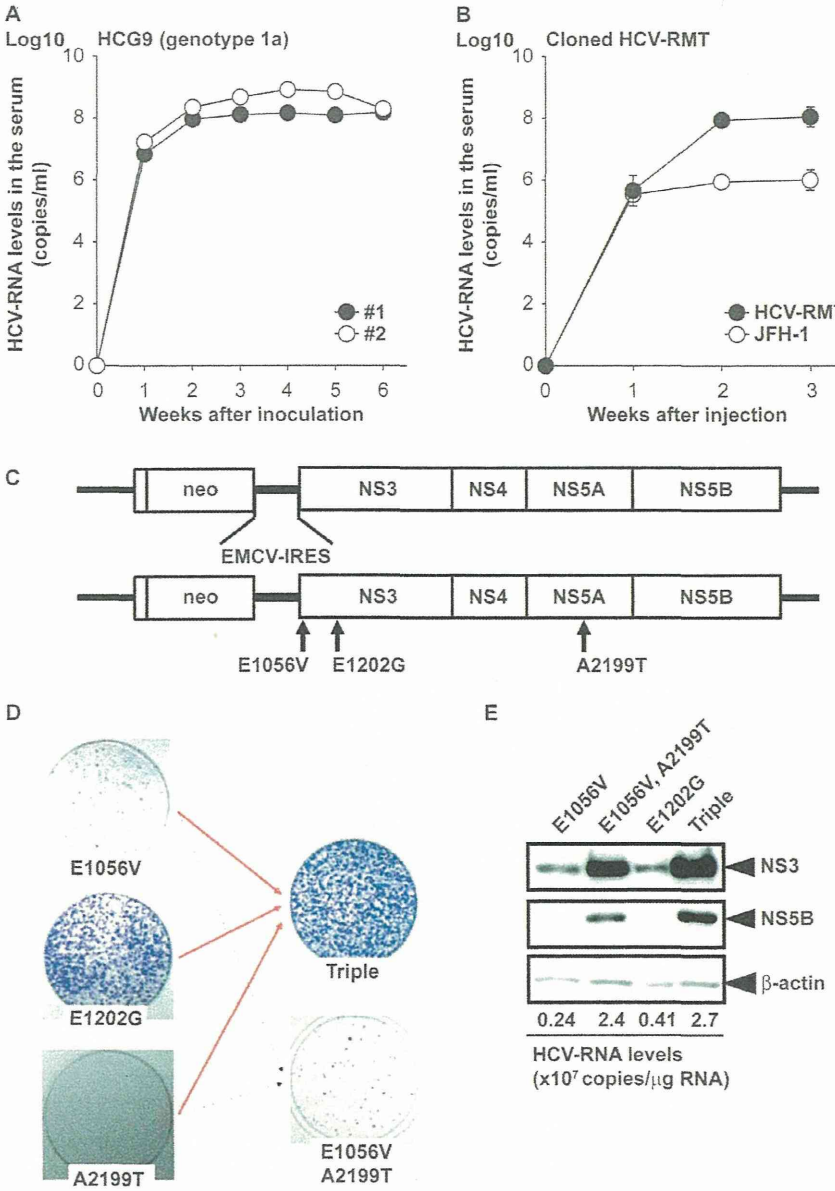

Figure 1. Basic characteristics of the HCV-RMT clone. Change in HCV copy number in chimeric mice. (A) Two mice were intravenously infected with 10 μl patient serum HCG9. (B) Three mice per group were directly injected with 30 μg HCV RNAs of the HCV-RMT strain or the JFH-1 strain into the liver. Data are indicated as the mean ± S.D. (C) Schematic representation of construction of the replicon and the sites of adaptive mutations. (D) *Colony formation assay of replicon clones with adaptive mutations. Each RNA (1 μg) was electroporated into HuH7-K4 cells.* (E) *Western blot analysis* of replicon cells. Each culture of replicon RNA-electroporated cells was maintained and passaged with G418 selection for 2 weeks. Cell lysates (10 μg) were loaded onto an SDS-PAGE gel.
doi:10.1371/journal.pone.0082527.g001

In vivo replication abilities of HCV-RMT derivatives were inversely proportional to their *in vitro* abilities

We assessed the *in vivo* replication abilities of HCV-RMT derivatives carrying combinations of the three adaptive mutations using chimeric mice with humanized liver. *In vitro*-generated HCV genomic RNAs were injected directly into the livers of the chimeric mice during abdominal surgery. Mice were monitored for amounts of genomic RNA in the blood once a week for 6 weeks, and virus titers in the livers were quantified after sacrifice of the mice. As shown in Figure 4A, in contrast to the vigorous *in vitro* replication ability, the clone that was most active *in vitro*, HCV-RMTtri, showed no evidence of replication *in vivo*, whereas the wild type showed replication that was comparable to the parental virus in the patient's serum, HCG9. In addition, the double mutant (E1056V, A2199T), which showed little replication *in vitro*, showed a similar replication ability as the wild-type clone. The most positively influential adaptive mutation (E1202G) seemed to

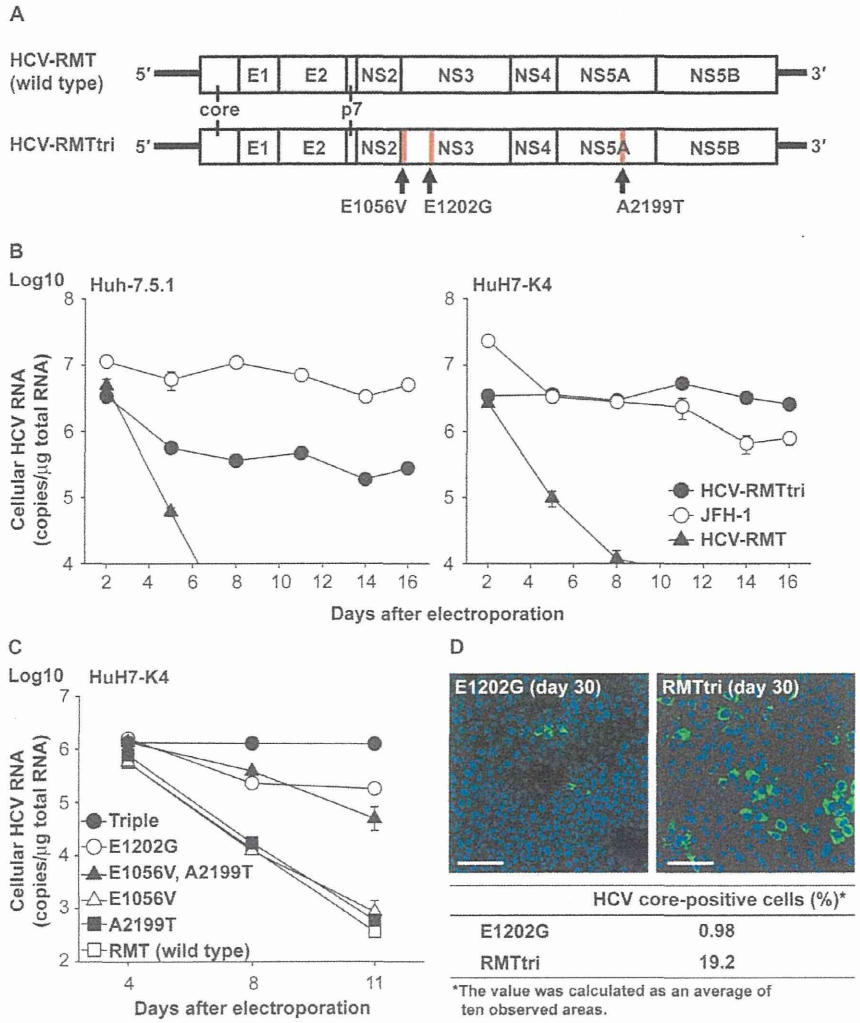

Figure 2. *In vitro* replication ability of HCV-RMT derivative genomes. (A) Schematic representation of construction of the HCV genome and the sites of adaptive mutations (red bars). (B) Electroporation of the generated HCV-RNA genomes of wild-type HCV-RMT (closed triangles), HCV-RMT with triple mutations (HCV-RMTtri; closed circles), and the JFH-1 strain (open circles) into Huh-7.5.1 or HuH7-K4 cells. The experiments were carried out in duplicate. (C) Comparison of the *in vitro* replication ability of each HCV-RMT derivative in HuH7-K4 cells. The experiments were carried out in duplicate. Wild type: open squares, E1202G: open circles, E1056V: open triangles, A2199T: closed squares, E1056V and A2199T: closed triangles, triple mutations: closed circles. (D) Immunostaining for the HCV core protein in HCV-RNA-electroporated cells. Scale bar = 100 μm. The percent of HCV core protein-positive cells (%) was calculated as an average of ten observed areas.
doi:10.1371/journal.pone.0082527.g002

hamper its *in vivo* replication ability. Quantification of HCV genomic RNA in liver (Figure 4B, C) showed a conserved serum/liver ratio among HCV-RMT derivatives. Thus, the blood titers directly reflected the titers in liver, although the ratio was considerably different than that of JFH-1. Table 1 shows the replication abilities of derivatives and JFH-1 both *in vitro* (HuH7-K4 cells) and *in vivo* (chimeric mice), clearly showing the inversely proportional relationship between them, including the replication ability of JFH-1, which corresponds to data in a previous report [29].

Discussion

In this report, we investigated many types of HCV replication systems using our newly cloned HCV-RMT.

The first type is replication in cultured cells as an authentic replicon construction. This system only depends on the ability to replicate in cells. HCV-RMT was the first genotype 1a clone that could be established in authentic replicon cells without artificially introduced adaptive mutations that are required by H77 [30,31], although the three spontaneously occurring mutations (E1056V, E1202G, and A2199T) are not novel [11,31]. Among the mutants with single mutations or a combination of these three adaptive mutations, the amounts of HCV genome and viral proteins did not reflect the colony-forming abilities (Figure 1D, E). The A2199T mutation, which least affects the colony-forming ability (no stable replicon cell line was established with this single mutation). However, combination of mutations including A2199T, triple (E1056V, E1202G and A2199T) and double (E1056V and